Polymer Chemistry

PAPER

View Article Online
View Journal | View Issue

Cite this: *Polym. Chem.*, 2014, **5**, 2309

A new strategy of post-polymerization modification to prepare functionalized poly(disubstituted acetylenes)†

Yuan Gao,[a] Xiao Wang,[a] Li Tong,[a] Anjun Qin,[a] Jing Zhi Sun*[a] and Ben Zhong Tang*[ab]

Two disubstituted acetylenes bearing a vinyl group at one end (**M1** and **M2**) were synthesized and polymerized by WCl_6–Ph_4Sn catalyst. The expected poly(disubstituted acetylenes) PDSAs (**P1** and **P2**) were obtained in high yields. Both **P1** and **P2** have reactive vinyl groups on their side chains, thus they were used as precursors to be subsequently modified with a mercapto compound through the thiol–ene click reaction to produce the novel PDSAs (**P1S** and **P2S**) in good yield. The chemical structures of the polymers were carefully characterized by standard spectroscopic methods such as gel permeation chromatography (GPC), NMR, NMR and FTIR techniques, and satisfactory data were collected. The post-polymerization modification of **P1** took a long reaction time (3 days) to convert **P1** to **P1S** because the ene-functionality at the end of side chain of **P1** links to a saturated alkyl segment. By using an activated ene-functionality (α,β-unsaturated vinyl), the modification of **P2** to **P2S** took only 1 day under mild conditions. Moreover, the activated end-ene group allowed the post-polymerization modification of **P2** by Michael addition, which was confirmed using butylamine as the representative amine compound and the characterization data indicated the validity of the expected **P2N**. The thermal analysis results indicated that the modified polymers were highly stable thermally with a decomposition temperature over at least 240 °C, except for **P2N**, which showed lower stability due to unstable imine groups. Meanwhile, it was found that the modified polymers **P1S** and **P2S** were fluorescent and showed similar emission efficiency to their precursors **P1** and **P2**. These results indicated that the thiol–ene click reaction and Michael addition reaction are accessible routes for post-polymerization modification to generate novel functional PDSAs.

Received 28th August 2013
Accepted 24th November 2013

DOI: 10.1039/c3py01164j

www.rsc.org/polymers

Introduction

Functionalization is the main use of polyacetylene-related polymers nowadays. A variety of functions, including photoconductivity, gas permeability, liquid crystal properties, polymer chain chirality, and inorganic-hybridization ability have been successfully incorporated into polyacetylene derivatives.[1–10] As a matter of fact, most of these functions were realized by the polymerization of monosubstituted acetylenic monomers, because Rh-based catalysts, which are tolerant to various polar functional groups in monomers and different solvents, can only catalyze the polymerization of monosubstituted acetylenic monomers.[1,2] It has been demonstrated that poly(disubstituted acetylenes) (PDSAs) or disubstituted polyacetylenes (PAs) prepared by polymerization of disubstituted acetylene monomers possess higher thermal and chemical stability and a greatly enhanced fluorescent emitting property in comparison to their counterpart mono-substituted PAs. However, the synthesis of PDSAs is heavily limited by the fact that the catalysts for the preparation of PDSAs are intolerant of polar functional groups such as hydroxyl, carboxyl, and amine. Consequently, the species of functional PDSAs are rare and the exploration of proper synthetic routes is of fundamental significance.

Post-polymerization modification is a powerful tool that has been widely used in the production of functional polymers.[11] For functional polyacetylenes, early work can be traced back to the preparation of primary amine-functionalized PDSAs by the hydrolyzation of phthalimide side groups with hydrazine.[12] This route was used for the synthesis of other primary amine-functionalized PDSAs, which were applied in the fabrication of liquid crystalline, light emission and fluorescent patterning

[a]*MOE Key Laboratory of Macromolecular Synthesis and Functionalization, Department of Polymer Science and Engineering, Zhejiang University, Hangzhou 310027, China. E-mail: sunjz@zju.edu.cn; Fax: +86-571-87953734; Tel: +86-571-87953734*

[b]*Department of Chemistry, Jockey Club Institute for Advanced Study, Institute of Molecular Functional Materials, State Key Laboratory of Molecular Neuroscience, Division of Biomedical Engineering, The Hong Kong University of Science & Technology, Clear Water Bay, Kowloon, Hong Kong, China. E-mail: tangbenz@ust.hk; Fax: +86-852-2358-7375; Tel: +86-852-2358-1594*

† Electronic supplementary information (ESI) available: ^{13}C NMR spectra of **M2**, **P2** and **P2S**, fluorescence changes of **P1**, **P2**, **P1S** and **P2S** with water fraction. See DOI: 10.1039/c3py01164j

polyacetylene–perovskite hybrids.[13,14] At the same time, Li and colleagues reported the Pd-catalyzed post-polymerization modification of PDSA bearing 4-iodophenoxy side groups, which offered ready access to soluble functional disubstituted PAs containing reactive apolar diarylethynyl and polar pyridyl and amido units.[15] In 2011, Theato's group pioneered work employing the activated ester strategy to modify the side chains of polyacetylenes. The post-polymerization reactions of the reactive polymers and copolymers with amines showed that the reactions proceeded quantitatively under mild conditions even with aromatic amines.[16] This triggered us to synthesize different polyacetylenes with tunable structures and properties such as hydrophobic, hydrophilic and amphiphilic property, and right-handed and left-handed helicity.[17] Recently, our group carried the work a step further to PDSAs and a series of functional disubstituted polyacetylenes with chiral moiety and hydroxyl and carboxyl groups in high yields.[18] Meanwhile, Theato and colleagues carefully investigated the effect of the position of the ester moiety on phenyl ring (*ortho*- and *meso*-isomers) on the reactivity towards different amines.[19] They found that thin films fabricated from these kind of polymers could be photopatterned by irradiating with UV light, and by using the activated esters as reactive sites, the patterned films could be further modified by functional amines to construct optical sensors.[20]

The activated ester strategy offers a facile and efficient synthetic route to PDSAs with tunable structures and functions. But amines have to be employed in the post-polymerization reaction and this limits the species of reactive molecules that can be used for the functionalization. Recently, click chemistry has evoked tremendous research efforts to design and synthesize versatile polymers such as block-copolymers, graft-copolymers, polymer brushes, dentritic and hyperbranched polymers.[21–25] Besides activated ester, the introduction of other click chemical reactions into the post-polymerization modifications of PDSAs should expand the species of modifiers and derive a more plentiful supply of functional polymers. Herein, we demonstrate our attempt to use thiol–ene click chemistry and Michael addition reaction in the preparation of post-functionalized PDSAs.

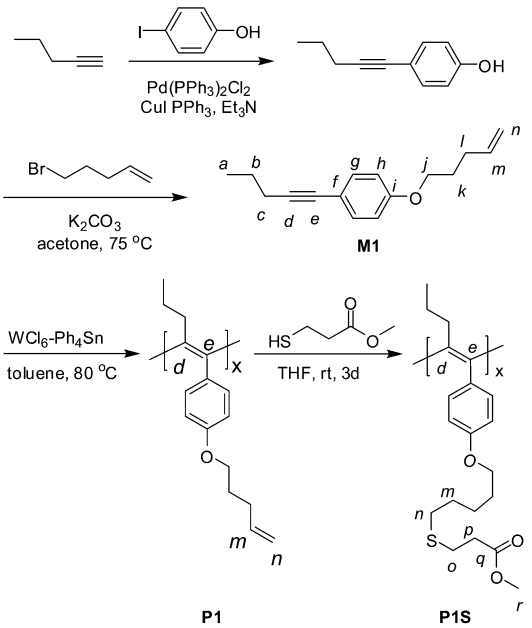

Scheme 1 Synthetic route to poly(disubstituted acetylene) with reactive end-vinyl groups (**P1**) and its derivative (**P1S**) after thiol–ene post-polymerization modification. The H and C atoms in the monomer (**M1**) and the repeat units of **P1** and **P1S** are labelled with letters in alphabetic order, some of the letters in **P1** and **P1S** are omitted for clarity.

Results and discussion

Polymerization of disubstituted acetylenes with end-capped enes

The first synthetic route to PDSAs containing end-capped vinyl functionality is shown in Scheme 1 (the experimental details and characterization data are included in Experimental section).

Disubstituted acetylene derivative with propyl and 4-phenol was prepared by Sonagashira condensation between 1-pentyne and 4-iodophenol. The disubstituted acetylene monomer **M1** was obtained in high yield of 88% by the reaction of the derived 1-(4′-phenol)-pentyne with 5-bromo-1-pentene. **M1** was characterized by standard spectroscopic methods, from which satisfactory analytical data were collected.

Relying on our previous works on the polymerization of disubstituted acetylenes,[18,26,27] the polymerization of **M1** was carried out in the presence of WCl_6–Ph_4Sn catalyst system at 80 °C in toluene solution. The experimental results indicated that the polymerization proceeded smoothly and the polymer (**P1**) was derived in an acceptable yield (32.8%) and moderate molecular weight ($M_w \sim 18\,000$) with the polydispersity index (PDI) of 1.9.

The chemical structure of the derived polymer **P1** was well-characterized by spectroscopic methods of ^{1}H NMR, ^{13}C NMR and FTIR. The ^{1}H NMR spectra of polymer **P1** and its monomer **M1** are shown in Fig. 1 as examples. In Fig. 1A, the chemical shift corresponding to each proton on **M1** is clearly assigned. After polymerization, all peaks of the chemical shifts become broadened. This change is rationally associated with the fact that a given unit of a polymer chain cannot move freely in solution because it must drag along the chain to which it is attached and weave its way inside the polymer coil. Since the phenyl and propyl groups are closely attached to the polyene main chain, the protons on these two moieties are displayed as more broadened and weakened. On the contrary, the protons on the pentenoid moiety show more clearly resolved peaks due to the separation of the phenyl between the pentenoid and polymer main chain. In addition, the polymerization has consumed the C≡C triple bond in **M1** and transformed it to C=C double bond that is in conjugation with the phenyl in **P1**. This change in the chemical environment leads to an up-shift of the protons on the phenyl from δ 7.35 (**M1**, Fig. 1A) to around 6.80–6.33 ppm (**P1**, Fig. 1B). Moreover, the protons on the ene-moiety show little change in their chemical shifts before and after polymerization. This indicates that the polymerization has not damaged the functional C=C double bonds.

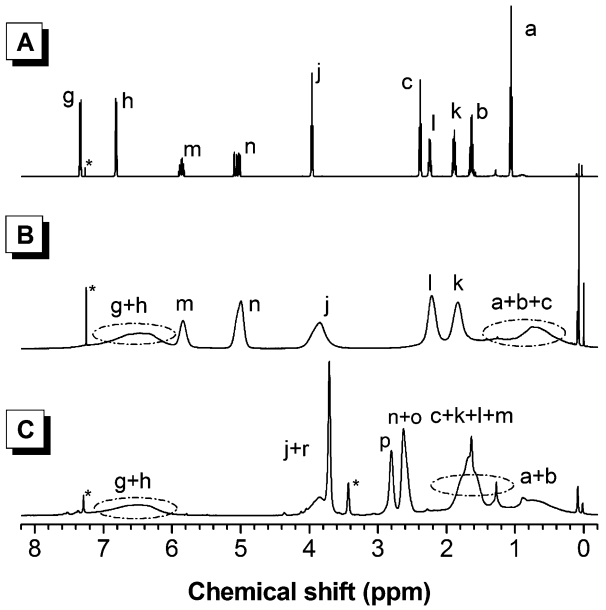

Fig. 1 ^{1}H NMR spectra of the disubstituted acetylene monomer (M1) and its polymers (P1 and P1S). The letters shown beside the peaks correspond to the structures in Scheme 1.

The ^{13}C NMR spectra of **M1** and **P1** provide further evidence to prove the polymerization. Comparing the chemical shifts for carbon atoms shown in Fig. 2, the chemical shifts of δ 88.7 and δ 80.7 are assigned to the carbons of d and e at the C≡C triple bond in **M1**. They have totally disappeared in **P1**. Meanwhile, the significant broadened resonance peaks for vinylidene groups appear at around δ 130 and 114 ppm. These signal changes suggest the formation of the polyene backbone of **P1**. Besides, the peaks of vinyl group in the side chain (peaks m and n, Fig. 2) still exist and show no shift, indicating that the end vinyl groups have been perfectly preserved during the polymerization.

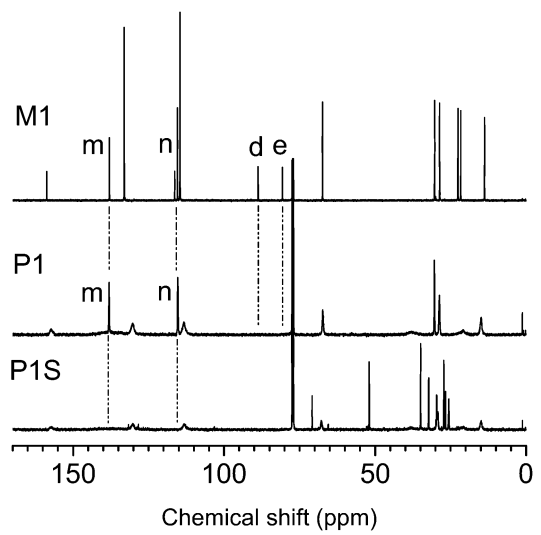

Fig. 2 ^{13}C NMR spectra of the disubstituted acetylene monomer (M1) and its polymers (P1 and P1S). The letters shown beside the peaks correspond to the structures in Scheme 1.

Fig. 3 displays the FTIR spectra of **M1**, **P1** and **P1S**. All of them have three common absorption features, which are the characteristic breathing bands for the phenyl skeleton that appear at around 1605 and 1508 cm^{-1}, and δ_{C-H} for 1,4-disubstituted phenyl that appears at around 831 cm^{-1}. The presence of these three bands confirm the presence of phenyls. The substitutions of the two protons of acetylene with carbon atoms render the C≡C triple bond in the disubstituted acetylene (*e.g.* **M1**) slowly IR-active. This is quite different from the monosubstituted acetylenes, which show the asymmetric stretching bands of C≡C triple and ≡C–H single bond at around 2140–2100 and 3330–3270 cm^{-1}, respectively. Nevertheless, the polymerization has transformed C≡C triple bond in **M1** to C=C double bond in **P1**, thus the absorption features associated with C=C bonds can be used to investigate the polymerization. For **M1** (Fig. 3A), the peak at around 1605 cm^{-1} can be also assigned to the C=C stretching band. For **P1** (Fig. 3B), this peak becomes broadened. This resulted from the better conjugation between the phenyl groups and C=C double bonds, implying the formation of the polyene backbone. The appearance of the sharp and moderate absorption band at around 916 cm^{-1} indicates the presence of unreacted –CH=CH$_2$ groups in both **M1** and **P1**.

Post-polymerization modification of P1 with methyl-3-mercaptopropanoate

The synthetic route of the post-polymerization modification of **P1** is presented in Scheme 1. The thiol–ene reaction was

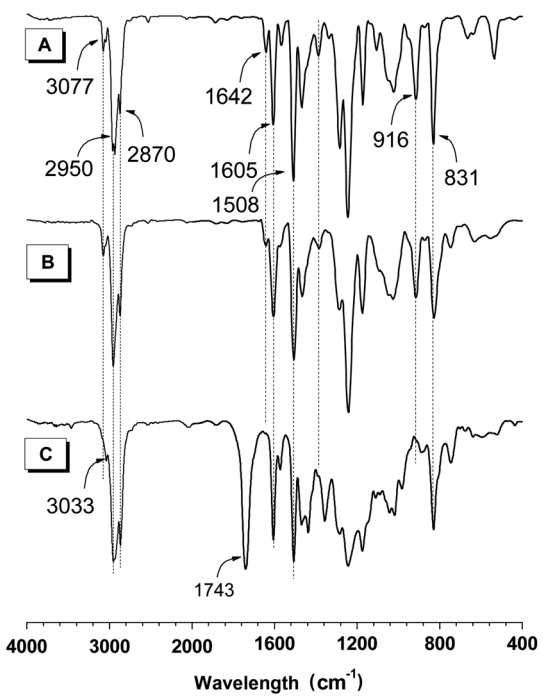

Fig. 3 FTIR spectra of M1, P1 and P1S. Part of the characteristic absorption bands are labelled with wavenumbers.

conducted in tetrahydrofuran solution at room temperature. Without the addition of any radical initiators, the reaction went on slowly and the modified polymer **P1S** was derived in good yield, 86.1%, after 3 days. The experimental details and characterization data are summarized in the Experimental section. By comparing the FTIR spectrum of **P1S** with that of **P1**, changes in the spectral features can be observed. The conspicuous absorption band at 1743 cm^{-1} denotes the existence of an ester group. This is solid proof of the successful attachment of methyl-3-mercaptopropanoate onto **P1** side chains. Meanwhile, the characteristic stretching band of –CH=CH_2 skeleton ($\delta_{C-H} \sim 910$ cm^{-1}, in plane) is observed for **P1**, but it disappears in the FTIR spectrum of **P1S** (Fig. 3B and C). This observation implies that the attachment of methyl-3-mercaptopropanoate onto **P1** side chain is associated with the consumption of the –CH=CH_2 moieties of **P1**, which can be ascribed to the thiol–ene addition in the present case. It is noticed that, comparing the FTIR spectra of **P1** with **P1S**, the absorption bands (between 1650 and 1500 cm^{-1}) underwent trivial changes after reaction for 3 days, suggesting that the C=C double bonds in the polyene main chain have not been attacked by the thiol group.

The ^{1}H NMR spectrum of **P1S** (Fig. 1C) reveal more information about the thiol–ene click reaction between methyl-3-mercapto-propanoate and **P1**. The peaks at δ 5.84 and δ 4.99 ppm are assigned to the protons on the vinyl group of the **P1**'s side chain (m and n, Fig. 1B) but they vanished in the ^{1}H NMR spectrum of **P1S** (Fig. 1C). Coincidentally, a group of new peaks appear at around δ 3.68, 2.78, 2.60, and 1.31 ppm. The peak at δ 3.68 ppm originates from the resonance of the methyl of the propanoate moiety. The peaks at δ 2.78, 2.60, and 1.31 ppm can be associated with the resonance of protons m, n and o, p. The changes in chemical shifts of protons m and n mean that the alkenyl protons on the ene-groups have been converted to alkyl protons. Due to the large chemical shift scope, the ^{13}C NMR spectra of **P1** and **P1S** (Fig. 2) offer higher resolution pictures to display the changes of resonant peaks for different protons. Peaks d (δ 115 ppm) and e (δ 138 ppm) disappear in Fig. 2B, but emerge in Fig. 2C at 25 and 27 ppm, respectively, indicating the transition from alkenyl to alkyl carbons. The appearance of peaks at δ 35, 71, 172 and 52 ppm (assigned to carbon atoms of o, p, q and r, respectively) in Fig. 2C also indicate the modification of **P1** by thiol compound. Finally the two mound-like features in Fig. 1C, ranging from 7.60 to 7.00 ppm and 1.00 to 0.30 ppm are assigned to the resonance of protons on phenyl and propyl, respectively. They hold constant in shape and size in both **P1** and **P1S**, because the thiol–ene click reaction has no influence on the phenyl and propyl moieties.

Due to the long reaction time and excess amount of methyl-3-mercapto-propanoate used in the post modification, three possible thiol–ene click reaction paths (i), (ii), and (iii) can be expected, as shown in Scheme 2. To quantitatively confirm that the thiol–ene click reaction only occurs to the side chain but not to the polyene main chain of **P1**, we calculated the integral of the proton peaks from the ^{1}H NMR spectra of **P1S**. If the thiol–ene click reaction occurs only to the side chains (i), the ratio of the different protons could be calculated according to the equation of (g + h) : (j + r) : p : (o + n) : (b + c + k + l + m) : a. If the

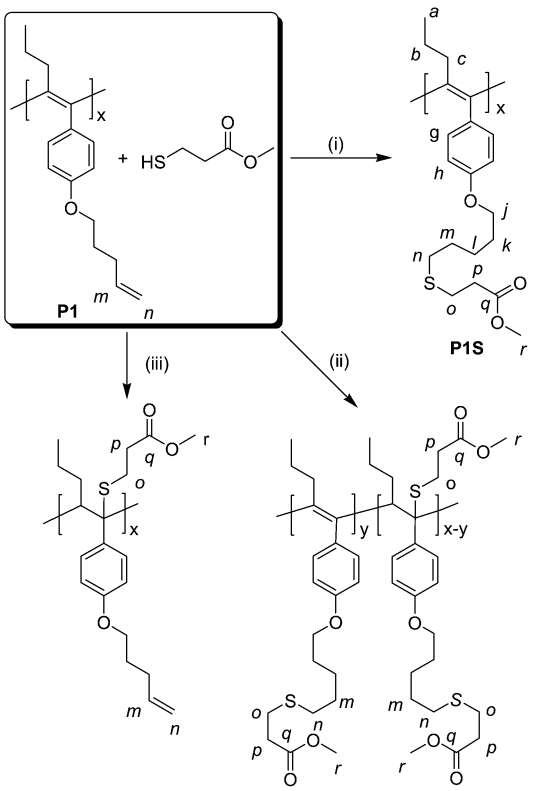

Scheme 2 Possible reaction paths of the thiol with C=C bonds in P1.

thiol–ene click reaction occurs to both the main and side chains (ii), the ratio of the different protons could be calculated by the equation (k + l) : [j + (1 + Δ)r] : (1 + Δ)p : [(1 + Δ)o + n] : (b + c + k + l + m) : *i*, where Δ is the fraction of methyl-3-mercapto-propanoate that reacts with the polyene main chain. Route (iii) can be directly denied because the ^{1}H and ^{13}C NMR spectra (Fig. 1C and 2C) show that the peaks assigned to the protons m and n have largely disappeared. The calculation shows that the ratio of different protons in Fig. 2C is (k + l) : (h + r) : t : (x + d) : (b + c + f + g + e) : a = 3.79 : 5.00 : 2.27 : 3.99 : 9.96 : 4.06 ≅ 4 : 5 : 2 : 4 : 10 : 4. This result is in excellent agreement with the result expected by route (i) shown in Scheme 2, where the theoretical ratio of relevant protons of **P1S** is (g + h) : (j + r) : p : (o + n) : (b + c + k + l + m) : a = 4 : 5 : 2 : 4 : 10 : 3. The excess amount of proton *a* for the experiment result may come from the integral deviation of the area of proton *a* due to the uneven base line. Therefore, we can reach the conclusion that the thiol–ene click reaction occurs only to the side chains of **P1** to produce the wanted post-polymerization modified **P1S**.

Amelioration of the efficiency of the post-polymerization modification

The post-polymerization modification of **P1** with thiol-compound methyl-3-mercaptopropanoate needs 3 days. It is not as efficient as our expectation of the thiol–ene click reaction, although the reaction proceeded under mild conditions. Thus we modified the structure of the monomer by replacing the 1-pentene with an acryloyl moiety, since the ethene group is

activated in the α,β-unsaturate ketone structure. This modification led to **M2** (Scheme 3) in a high yield of 82%. The structure of **M2** was characterized by standard spectroscopic methods and satisfactory analysis data were obtained (see Experimental section).

The polymerization of **M2** was carried out under the same conditions as those applied to **M1**. The experimental results demonstrated that the polymerization proceeded efficiently and that the polymer (**P2**) was derived in a better yield (47.8%) and a higher molecular weight ($M_w \sim 37\,000$) with a PDI of 2.2. The post-polymerization modification upon the thiol–ene reaction between methyl-3-mercaptopropanoate and **P2** was conducted in THF solution at room temperature (Scheme 3). The modification was finished in 1 day and the polymer **P2S** was derived in a yield of 100% without the addition of any radical initiators. The shorter reaction time and higher yield together validated the success of the modified synthetic route.

To confirm that the structures are the expected polymers, the spectroscopic techniques of FTIR, ^{1}H NMR and ^{13}C NMR have been used to characterize their structures. FTIR spectra of **M2**, **P2** and **P2S** are shown in Fig. 4. The strong band at around 1740–1760 cm^{-1} is assigned to the stretching band of C=O in the ester group ($\nu_{C=O}$), and it appears in all the spectral lines of **M2**, **P2** and **P2S**. There is a shoulder of this band for **P2S** due to the existence of two kinds of ester groups in the **P2S** macromolecules. In comparison in the spectra of **M2**, **P2** and **P2S** it can be seen that the absorption band at around 900 cm^{-1} (for –CH=CH_2) is owned by both **M2** and **P2**, but it disappears in the spectrum of **P2S**. The changes in the features $\nu_{C=O}$ and δ_{C-H} for –CH=CH_2 suggests that methyl-3-mercapto-propanoate has been added onto the side chains of **P2**, and the expected post-polymerization modification has been achieved.

Further confirmation of the successful post-polymerization modification is revealed by the ^{1}H NMR spectra of **P2** and **P2S** (Fig. 5). The peaks at δ 6.54, 6.28, and 5.94 ppm are assigned to the protons on the vinyl group of the **P2** side chain (m and n, Fig. 5B). They have disappeared in the ^{1}H NMR spectrum of **P2S** (Fig. 5C), indicating that they had been exhausted in the thiol–ene click reaction. A new peak appears at 3.70 ppm in the ^{1}H NMR spectrum of **P2S**, and this can be ascribed to the protons on the –CH_3 group of the methyl-3-mercaptopropanoate. The other two new peaks at δ 2.86 and 2.66 ppm are assigned to the protons on –CH_2–S–CH_2– and –CH_2–C=O groups, respectively. Due to the rigidity-induced low solubility of the polyene main chain, the protons on the propyl and phenyl groups, which attach directly to the main chain, manifest as weak, blunt and featureless resonant peaks.

The ^{13}C NMR spectra of **M2**, **P2** and **P2S** have been measured (Fig. S1†). The results show the disappearance of the vinyl group of P2**S** compared to P2, though the signals were not clear due to the low solubility of **P2S**. The available FTIR and ^{1}H NMR

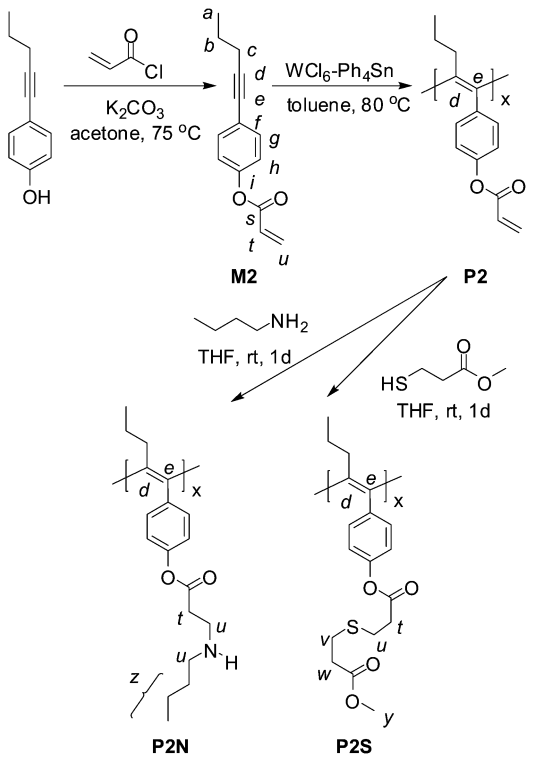

Scheme 3 Synthetic route to P2 through polymerization of M2 and post-polymerization modification of P2 to P2S and P2N through thiol–ene click reaction and Michael addition reaction. The H and C atoms in M2 and the repeat units of P2, P1S, P2N are labelled with letters in alphabetic order, some of the letters in the polymer structures are omitted for clarity.

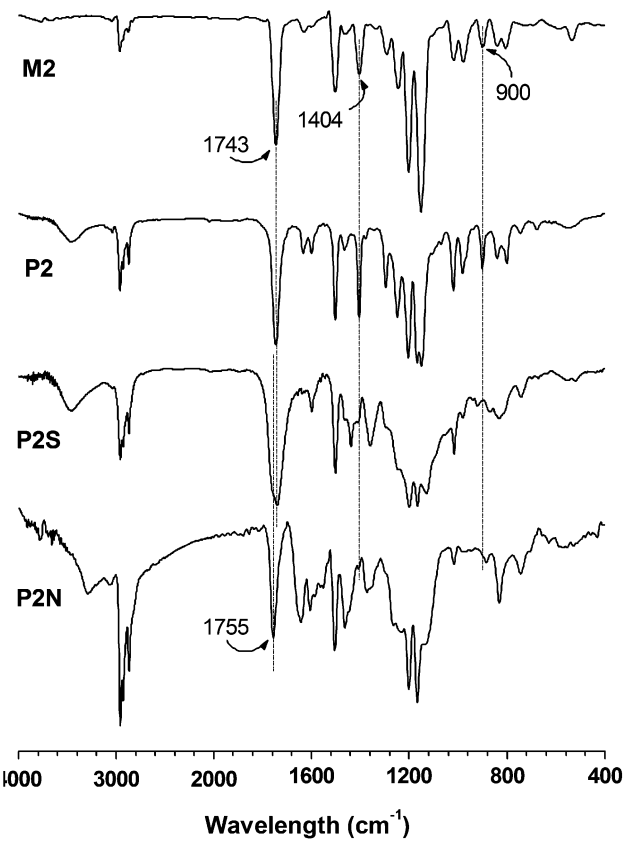

Fig. 4 FTIR spectra of M2, P2, P2S and P2N. Some characteristic absorption bands used for discussion are labelled with wavenumbers.

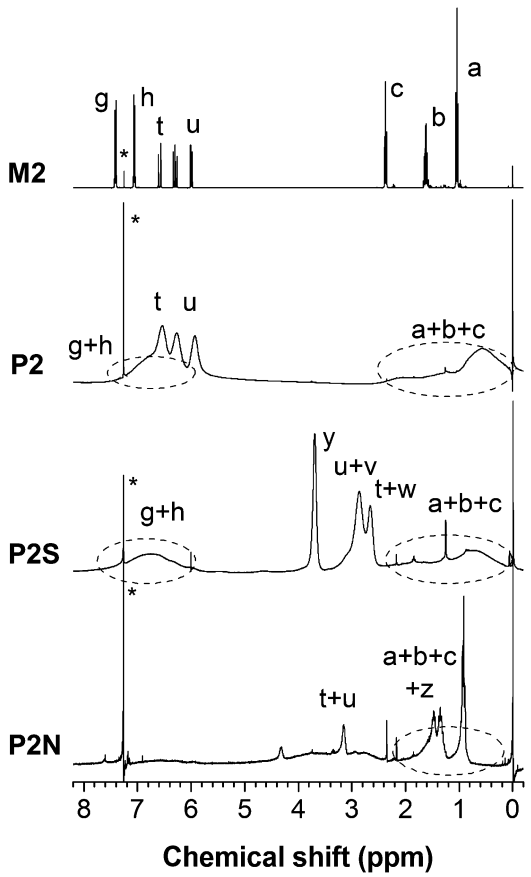

Fig. 5 ^{1}H NMR spectra of M2 and its polymers (P2, P2S and P2N). The letters beside the peaks correspond to the protons in Scheme 3.

spectra, nevertheless, are sufficient for us to draw the conclusion that both polymerization of **M2** (**M2** to **P2**) and the post-polymerization modification of **P2** (**P2** to **P2S**) have been successfully realized.

Post-polymerization modification of P2 through Michael addition reaction

Besides the thiol–ene click reaction, the α,β-unsaturate ketone can efficiently react with amine under mild conditions. This reaction is named as Michael addition and has been widely used to synthesize various poly(amido amines).[28,29] Here we used *n*-butamine as representative to demonstrate the feasibility of the post-polymerization modification of **P2** with amine-compound (Scheme 3). The experiment procedures are similar to those described for **P2S**, and the reaction time was also set to 1 day. But dissimilarly, the purified **P2N** cannot dissolve in common solvents, thus the structure characterization of **P2N** was limited. To obtain a ^{1}H NMR spectrum of **P2N**, we conducted the post-polymerization modification of **P2** with *n*-butylamine in deuterated chloroform solution. After reaction for 1 day, the recorded ^{1}H NMR spectrum of the mixture is shown as Fig. 5. The disappearance of the resonance peaks at δ 6.54, 6.28, and 5.94 ppm (–C*H*=C*H*$_2$ for **P2**) suggests that the ene-functionalities on the side chains of **P2** have been used up in the modification reaction. Meanwhile, three new resonance peaks at δ 3.16, 1.48, 1.35, and 0.92 ppm appear, which are ascribed to the protons on newly added butyl.

FTIR spectroscopy was used to study the post-polymerization modification process, because it works well for insoluble samples. As shown in Fig. 4 (**P2N**), the sharp and strong band with a peak at 1755 cm^{-1} is assigned to $\nu_{C=O}$ of the ester group. In comparison to the $\nu_{C=O}$ band of **P2** appearing at 1743 cm^{-1}, there is a 12 cm^{-1} shift of wavenumber, which is induced by the conversion from α,β-unsaturate ester (vinyl, **P2**) to saturate ester (alkyl, **P2N**). In Fig. 4D, there is a weak band at around 3300 cm^{-1}, which is assigned to the stretching mode of the secondary amine ($\nu_{=N-H}$). It appears at the low wavenumber side of the typical $\nu_{=N-H}$ band and displays a broad shape, implying the formation of hydrogen bonds between different molecules. The appearance of this band suggests the absence of primary amine, otherwise a stronger absorption band in a double-peaked shape should exhibit at around 3400–3500 cm^{-1}. These features are proof to support the realization of the Michael addition reaction.

The most significant change between the spectra of **P2N** and **P2** is the disappearance of the absorption band at around 1404 cm^{-1}, which is a sign of the bending mode for the –CH=C*H*$_2$ moiety (δ_{C-H}, in plane). Meanwhile, the cogenetic bending mode at around 900–910 cm^{-1} (δ_{C-H}, out of plane) undergoes a synchronous change. The vanishing of the "out of plane" and "in plane" modes can be used as indicators to monitor how the Michael addition process proceeds. Time-dependent FTIR spectra of the **P2** and *n*-butylamine reactive mixtures are displayed in Fig. 6. By using the $\nu_{C=O}$ band as an inner calibration, the relative intensity changes for the "out of plane" and "in plane" modes can be observed. After reaction for 24 h, the out of plane mode of the –CH=C*H*$_2$ moiety became very weak, and extending the reaction time to 48 h led to little change in the spectrum. Thus, we chose 1 day as the acceptable reaction time. Altogether, the post-polymerization modification from **P2** to **P2N** has been realized.

Thermal stability

One of the advantages of the PDSAs over their monosubstituted counterparts is improved thermal stability. For example, the decomposition temperature (T_d, defined as the temperature at which the polymer loses 5% of its original weight) of poly(diphenylacetylene) is about 342 °C,[26] which is obviously higher than that of polyphenylacetylene (about 225 °C).[28] In our previous works, we prepared a series of PDSAs, and noticed that the derivatives of poly(1,2-diphenyl-acetylene) showed the highest thermal stability among the different PDSAs. Replacing a phenyl by an alkyl led to lowering of the thermal stability of the polymers, and the poly(1,2-dialkyl acetylenes) showed the lowest thermal stability.[29] This trend is also true in the present work. As revealed in Fig. 7, the T_d for **P1** is 381 °C. After the post-polymerization modification with methyl-3-mercapto-propionate, the T_d of **P1S** decreased to 312 °C, about a drop of 70 degrees in comparison with **P1**.

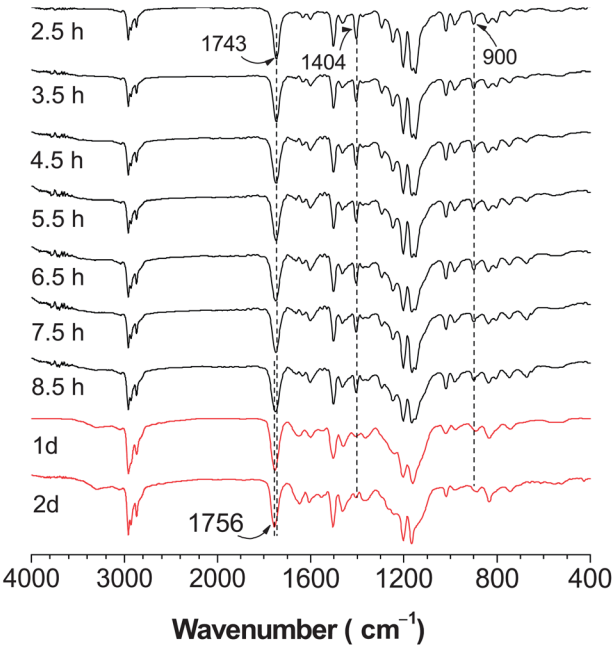

Fig. 6 Time-dependent FTIR spectra of the reactant mixture of P2 and *n*-butylamine. The characteristic bands for –CH=CH_2 and C=O groups are labelled with wavenumbers.

Similarly, the modification of **P2** with methyl-3-mercaptopropionate leads to **P2S**, which exhibits a more pronounced drop of T_d (242 °C) as compared to **P2**. Michael addition of *n*-butylamine to the side chains of **P2** resulted in **P2N**, which has a further lowered T_d (198 °C). Besides the introduction of alkyls into the polymer side chains, the decreased T_d from **P1** to **P1S** and from **P2** to **P2S** can be associated with the ethenyl group at the end of each polymer side chain. At an elevated temperature, thermal triggered crosslinking between the ethenyl groups takes place and renders the polymer improved thermal resistance. Similar thermal performance was observed for other polyacetylenes with vinyl-containing side chains.[26,30]

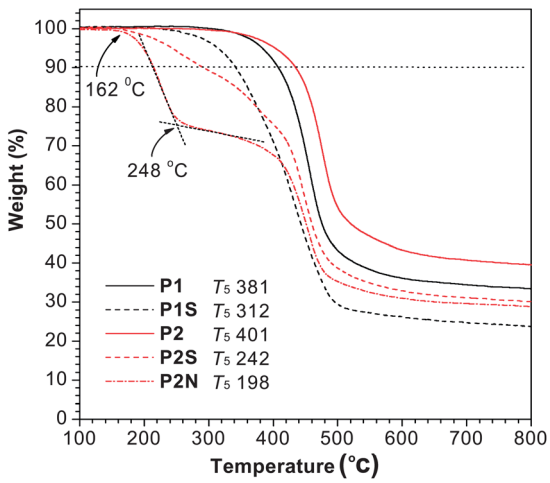

Fig. 7 TGA thermograms of P1, P1S, P2, P2S and P2N measured under a nitrogen atmosphere at a heating rate of 20 °C min^{-1}. T_5 denotes the temperature at which the sample loses 5% of its original weight.

A noticeable feature in Fig. 7 is that both **P1** and **P2** possess the highest residual weight at 800 °C in their corresponding modified structures (**P1S** and **P2S**, **P2N**), which can be considered as additional proof to confirm that the post-polymerization modification has been realized. Another feature is the distinct low thermal stability of **P2N**. **P2N** begins to lose its weight at around 162 °C, loses 25% of its original weight at around 248 °C, and then enters into a declining platform which is ended by a steep fall at around 415 °C. The low weight-loss temperature at 162 °C can be ascribed to the encapsulation of solvent molecules in **P2N**. The Michael addition reaction of the amine and ethenyl groups bestowed **P2N** with abundant secondary amines, which form intra- and inter-macromolecular hydrogen bonds. The formation of hydrogen bonds has been confirmed by both FTIR spectra (Fig. 5D and 6) and the indistinguishable chemical shifts in ^{1}H NMR spectrum (Fig. 4D), as well as the observed low solubility of **P2N**. The first drop between 162 °C and 248 °C is tentatively ascribed to the decomposition of **P2N** by losing the butylamine moiety in the polymer, because the reduction of this moiety from each repeat unit of **P2N** is in good agreement with the recorded 25% weight loss. After this transition, all samples show an identical temperature-dependent weight-loss, and this subsequent process is mainly associated with the decomposition of the polymer backbone.

The differential scanning calorimeter (DSC) data are shown in Fig. S2.† In the heating run, **P1** and **P2S** show wide indothermal peaks centered at around 90 °C and 95 °C respectively, and they disappear in the corresponding cooling process. Thus these two features can be associated with the sample processing history. Other polymers have no obvious transitions, as observed for their heating and cooling curves. These data further confirmed that the polymers are thermally stable.

Fluorescent properties

Another advantage of the PDSAs over their monosubstituted counterparts is their efficient emission properties. Due to the existence of deep exciton traps in the polyene backbone, both monosubstituted polyalkylacetylenes and polyphenylacetylenes are very weakly emissive in both solution and solid states.[1,31,32] Attaching fluorescent moieties onto the side chains of these two types of polymers can derive fluorescent polyacetylenes, but the emission efficiency is not high, because the emission from the fluorescent moieties on the side chains can be quenched by the polyene main chain for a considerable fraction.

In contrast, most of the PDSAs are highly emissive, and the best record of the quantum efficiency is as high as 98%.[33] In our previous works, we reported synthesis and fluorescent properties of a series of PDSAs bearing vinyl groups at the end of the side chains.[26,30] These polymers showed good processability, high emission efficiency and the ability to form the right fluorescent patterning. Herein, both **P1** and **P2** demonstrate similar properties to those reported in the literature. Progress in the

present work is to use **P1** and **P2** for post-polymerization modification to develop novel functional PDSAs.

The thiol–ene click reactions bring sulfur atoms into the modified polymers **P1S** and **P2S**, which may cause fluorescent quenching due to the well-known heavy atom effect. To examine the effect of post-polymerization modification on the fluorescent performance, we measured the fluorescence spectra of **P1**, **P2**, **P1S**, **P2S** in their dilute THF solutions, and the results are displayed in Fig. 8A. **P1** and **P1S** have identical emission features with a broad band and a maximum at 467 nm. **P2** and **P2S** show a similar broad emission band but the corresponding emission peaks appear at 476 and 463 nm, respectively. Accordingly their chemical structure, **P2** has the shortest side chains among **P1**, **P1S**, **P2** and **P2S**, thus the **P2** backbone should have the longest effective conjugation length due to the smallest hindrance between adjacent repeat units. After thiol–ene click modification, the side chains of **P2S** become longer. As a result, the polymer main chains take a more twisted conformation and the emission band undergoes a blue-shift. The fluorescence images of the four polymers in THF solution are set in Fig. 8A, we can see that the four polymers are all highly emissive, and only the **P2** solution shows a bluish-green emission. Fig. 8B displays the photographs of the fluorescence spectra of the casting films of the four polymers. All of them emit blue fluorescence and the peak wavelength locates at around 465 nm

Quantitative evaluation of the fluorescent property comes from the measurement of their quantum yield (Φ_F) in dilute THF solutions. Estimated by 9,10-quinine sulfate (54% in 0.1 N sulfuric acid), Φ_F value for **P1**, **P1S**, **P2** and **P2S** is 51.7%, 47.8%, 47.1% and 48.0%, respectively. These data are comparable to our previously reported results derived from other PDSAs.[18,26,30] More importantly, the data imply that the thiol–ene click reaction has a very weak impact on the fluorescence property of the modified products.

Generally, poly(disubstituted phenylacetylenes) possess a characteristic of aggregation-enhanced emission (AEE). The first AEE phenomenon was observed for poly(1-phenyl-1-octyne), whose Φ_F increased by about 2.5 fold when its solvent was changed from pure THF to a THF–water mixture containing 90% water.[34] As can be seen from Fig. 9, **P1**, **P1S**, **P2** and **P2S** also exhibit such an AEE behavior in THF–water mixtures with a low water fraction (f_W). By progressively increasing f_W in the THF–water mixture to 20%, the fluorescence intensity of **P1** enhances continuously. In this step, the THF–water mixtures are still relatively "good" solvents for the polymer chains, but the enhanced polarity drives partial hydrophobic chains to form aggregates. The aggregate formation restricts the rotation of the phenyl rings against the polyene backbone, which allows the polymer better emissivity. This is a common feature for many tetraphenylethene ($Ph_2C{=}CPh_2$) derivatives,[35,36] and the AEE is reasonable if the repeat unit ($P^1RC{=}CPhP^2$, where P^1 and P^2 are polyene chains) is considered as an analogue of the tetraphenylethene derivative. When more water is introduced into the solvent mixture, the THF–water mixtures become relatively "poor" solvents for the polymer chains, and the polymer chains aggregate into clusters at sizes of nanometers so that the solutions are still macroscopically homogeneous and visually transparent. Nevertheless, $P^1RC{=}CPhP^2$ is unequal to $Ph_2C{=}CPh_2$. The cluster formation allows close packing of the polymer segments, since $P^1RC{=}CPhP^2$ is not as rigid as $Ph_2C{=}CPh_2$, where the double bond is linked to four rigid phenyl groups. Consequently, fluorescence becomes partially quenched by the enhanced interchain interactions. Indeed, when the flexible alkyl side chains were replaced by the rigid phenyl groups, the more rigid poly(1,2-diphenylacetylene) derivatives had a more pronounced AEE performance and showed a monotonous enhancement of fluorescent intensity with the increase of water fraction.[26,34] When f_W is over 60%, the THF–water mixtures become non-solvent for the polymer, the solutions are so unstable that some flocci appear and the polymer aggregates can deposit on the walls of the quartz cell. Consequently, the measured data of fluorescence intensity are fluctuate hugely

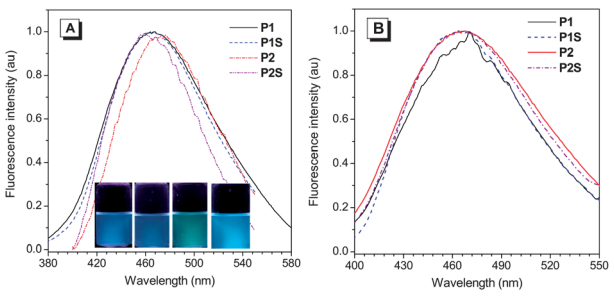

Fig. 8 Fluorescence spectra of **P1**, **P1S**, **P2** and **P2S** in THF solution (A) and cast film (B). Inset of A shows the fluorescent images of the solutions, from left to right correspond to **P1**, **P1S**, **P2** and **P2S**, respectively. Polymer concentration: 10 μM, Excitation wavelength: 280 nm.

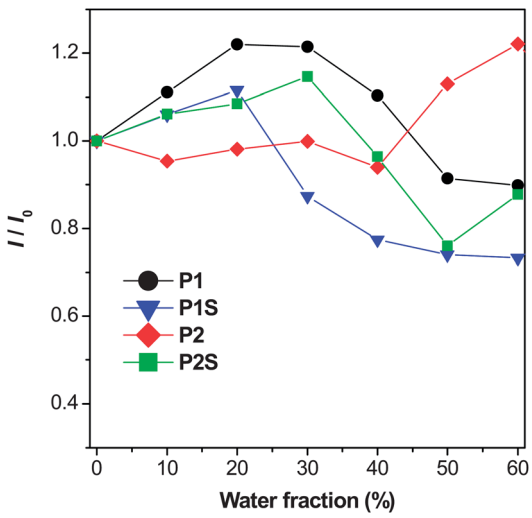

Fig. 9 Variation of the relative fluorescence intensity (I/I_0) of the modified PDSAs (**P1S** and **P2S**) and their precursors (**P1** and **P2**) in THF–water mixtures with different water fractions, where I and I_0 are the fluorescence intensity recorded for the samples in pure THF solution. Polymer concentration: 10 μM, excitation wavelength: 280 nm, water fraction was calculated by volume.

and arbitrarily. This trend is also true for the other three polymers (see Fig. S3†).

P1S, or the modified structure showed a similar fluorescent behavior to its precursor polymer **P1**. Increasing f_W from 0 to 20% leads to a 1.6 fold enhancement of the fluorescence intensity, and the intensity declines with further increasing f_W values. It is noticeable that, on one hand, the intensity decline of **P1S** is faster that of **P1**. And on the other hand, the fluorescence quenching of **P1S** is more intensive than that of **P1** when f_W is over 20%. These differences can be interpreted as following. The thiol–ene click reaction has extended the length of the side chains. This structural variation improves the flexibility of the side chains and makes the polymer segments, on one hand, easy to form regular packing, and on the other hand, makes it being propitious to the interchain electronic interactions. Thus pronounced fluorescence quenching has been observed for **P1S**.

P2 displays distinct fluorescent behaviors from **P1**. As shown in Fig. 9, the fluorescence intensity has little changes in a wide f_W range (from 0 to 40%). Further increasing f_W from 40% to 60% results in the enhancement of the fluorescence. This observation can be associated with the acrylate groups of **P2**. As discussed above, **P2** has the shortest side chains among the four polymers, the smallest hindrance between adjacent repeat units bestows **P2** backbone with the longest effective conjugation length. Thus **P2** emits bluish-green fluorescence (Fig. 8A). At the same time, the effectively conjugated backbone endues it with steady configuration and fluorescence. In addition, the polar ester groups on the side chains allow the polymer less sensitive to water content in the mixture solvent. At higher f_W, the fluorescence intensity boosts up because the aggregate formation restricts the rotations of the phenyl rings and avails the fluorescent emission. After attachment of a longer and hydrophobic chain to each repeat unit of **P2**, the fluorescent behaviors of the modified **P2S** come back to that of **P1** and **P1S**. The effect of the polar ester group (acrylate moiety) is manifested by the fact that the fluorescence decline of **P2S** occurred at relatively higher f_W.

Experimental section

Materials

4-Iodophenol, 1-pentyne, methyl-3-mercaptopropionate, WCl_6 were purchased from Acros. $PdCl_2(PPh_3)_2$ and Ph_4Sn were purchased from ABCR. 5-Bromo-1-pentene was purchased from Energy Chemical. Other chemicals used in this work such as sodium, triphenylphosphine, copper iodide, potassium carbonate, ammonium chloride, petroleum ether, ethyl acetate, methanol, dichloromethane (DCM), tetrahydrofuran (THF), triethylamine and toluene were purchased from Sinopharm. THF, toluene were distilled from sodium benzophenone ketyl under nitrogen in normal pressure. Triethylamine was distilled from calcium hydride. Other chemicals were used without stating.

Instruments

IR spectra were recorded on a Bruker VECTOR 22 spectrometer. ^1H and ^{13}C NMR spectra were measured on a Bruker ARX 500 spectrometer using $CDCl_3$ and *d*-DMSO as solvent and tetramethylsilane as internal standard. Thermal stability and thermal transition of the polymers were evaluated on a Perkin-Elmer Pyris thermogravimetric analyzer TGA 6 and a Perkin-Elmer DSC 7 instrument, respectively. Fluorescence spectra were recorded on a Perkin-Elmer spectrofluorometer LS 55. Weight-average (M_w) and number-average (M_n) molecular weights and polydispersity indexes (M_w/M_n) of the polymers were estimated in THF by a Waters Associated gel permeation chromatography (GPC) system. A set of mono-disperse polystyrene standards covering molecular weight range of 10^3 to 10^7 was used for the molecular weight calibration.

Monomer synthesis

The synthetic route of monomer **M1** and **M2** was shown in Schemes 1 and 3. The experimental procedures were given below.

1-(Pent-1-ynyl)-4-(pent-4-enyloxy)benzene (M1). Into a 250 mL two-necked round-bottom flask was added 1.118 g (5 mmol) 4-idiophenyl, 35 mg (0.05 mmol) $PdCl_2(PPh_3)_3$, 19 mg (0.1 mmol) CuI, 13 mg (0.05 mmol) PPh_3 and 30 mL triethylamine under nitrogen. 0.6 mL (6 mmol) 1-pentyne was injected into the flask after all chemicals were dissolved, then the mixture was stirred for 24 h. After filtered out the salt formed in the reaction, the solution was washed by saturated NH_4Cl aqueous solution to remove the triethylamine. Then the solution was extract with DCM and water. Combined the organic layer and washed with hydrochloric acid, brine and water. The result solution was dried over by magnesium sulfate and evaporated the solvent. The result crude product was added into a 100 mL one-necked flask with 2.07 g (15 mmol) K_2CO_3, 55 mL acetone and 0.6 mL (6 mmol) 5-bromo-1-pentene. The mixture was refluxed for 36 h at 75 °C. After removing the white salt in the system by filter and washing with acetone, the filtrate was condensed and the crude product was obtained. It was purified by column chromatography using petroleum ether as eluent. The pure product was a colorless liquid with a yield of 88%. ^1H NMR (500 MHz, $CDCl_3$), δ (TMS, ppm): 7.35 (d, 2H), 6.82 (d, 2H), 5.86 (m, 1H), 5.06 (m, 2H), 3.96 (t, 2H), 2.38 (t, 2H), 2.25 (m, 2H), 1.90 (m, 2H), 1.65 (m, 2H), 1.06 (t, 3H).^{13}C NMR (125 MHz, $CDCl_3$), δ (ppm): 158.7, 137.9, 133.1, 116.4, 115.4, 114.6, 88.7, 80.7, 67.4, 30.3, 28.6, 22.6, 21.6, 13.8. HRMS (*m*/*z*): calcd for $C_{16}H_{20}O$, 228.1514; found, 228.1515.

1-(Pent-1-ynyl)-4-acryloyloxy-benzene (M2). Into a 250 mL two-necked round-bottom flask was added 1.118 g (5 mmol) 4-idiophenyl, 35 mg (0.05 mmol) $PdCl_2(PPh_3)_3$, 19 mg (0.1 mmol) CuI, 13 mg (0.05 mmol) PPh_3 and 30 mL triethylamine under nitrogen. 0.6 mL (6 mmol) 1-pentyne was injected into the flask after all chemicals were dissolved, then the mixture was stirred for 24 h. After filtered out the salt formed in the reaction, the solution was washed by saturated NH_4Cl aqueous solution to remove the triethylamine. Then the solution was extract with DCM and water. Combined the organic layer and washed with hydrochloric acid, brine and water. The result solution was dried over by magnesium sulfate and evaporated the solvent. The result crude product was added into a 100 mL one-necked

flask with 2.07 g (15 mmol) K_2CO_3, 55 mL acetone and 0.41 mL (5 mmol) acryloyl chloride. The mixture was refluxed for 36 h at 75 °C. After removing the white salt in the system by filter and washing with acetone, the filtrate was condensed and the crude product was obtained. It was purified by column chromatography using petroleum ether as eluent. The pure product was a colorless liquid with a yield of 82%. ^{1}H NMR (500 MHz, $CDCl_3$), δ (TMS, ppm): 7.41 (d, 2H), 7.04 (d, 2H), 6.59 (m, 1H), 6.30 (m, 1H), 5.99 (m, 1H), 2.37 (t, 2H), 1.61 (t, 2H), 1.04 (t, 3H). ^{13}C NMR (125 MHz, $CDCl_3$), δ (ppm): 164.2, 149.8, 132.8, 127.9, 121.9, 121.6, 90.4, 79.9, 22.1, 21.3, 14.5.

Polymer synthesis

The polymerization reaction were all taken place under dried nitrogen using standard Schlenk technique, except the purification of the polymer. A typical procedure for the polymerization of **M1** is given below as an example.

Into a baked 10 mL Schlenk tube with a stopcock in the side arm was added 183 mg of **M1** under nitrogen. Then, 2 mL freshly distilled toluene was injected into the tube to dissolve the monomer. The catalyst solution was prepared in another tube by dissolving 16 mg (0.04 mmol) WCl_6 and 17 mg (0.04 mmol) Ph_4Sn in 2 mL freshly distilled toluene. The catalyst solution was aged at 80 °C for 15 min. Then the **M1** solution was transferred into the catalyst solution tube by a hypodermic syringe. The reaction mixture was stirred at 80 °C for 24 h. The solution was then cooled to room temperature, diluted with 5 mL of chloroform, and was added dropwisely in to 300 mL methanol under stirring through a cotton filter. The precipitate was allowed to stand overnight and then collected by filtration. The polymer was washed with methanol for several times and dried at room temperature to a constant weight. A light grey solid of **P1** was obtained with a yield of 32.8‰ GPC: M_w 18 000; M_w/M_n 1.9. ^{1}H NMR (500 MHz, $CDCl_3$), δ (TMS, ppm): 6.80–6.33, 5.84, 4.99, 3.85, 2.21, 1.83, 1.08–0.25. ^{13}C NMR (125 MHz, $CDCl_3$), δ (ppm): 157.3, 138.1, 135.0, 130.3, 115.4, 113.3, 67.4, 38.1, 30.4, 28.7, 20.8, 14.8.

P2 GPC: M_w 37 000; M_w/M_n 2.2. ^{1}H NMR (500 MHz, $CDCl_3$), δ (TMS, ppm): 7.10–6.50, 6.54, 6.28, 5.92, 1.04–0.25. ^{13}C NMR (125 MHz, $CDCl_3$), δ (ppm): 164.1, 149.2, 139.5, 131.8, 129.7, 120.4, 37.1, 20.8, 14.6.

Post-modification reaction

Thiol–ene click reaction. The post-modification reactions of **P1** and **P2** were all carried out under dried nitrogen using standard Schlenk technique, except the purification of the modified polymers. The thiol–ene click reaction between the thiol compounds and the reactive double bond in the side chains of the polymers was shown in Scheme 1. Typical experimental procedures for the preparation of **P1S** are given below as an example.

Into a 10 mL Schlenk tube with 45 mg (0.2 mmol) **P1** under nitrogen then dissolved in 2 mL freshly distilled THF. Methyl-3-mercaptopropanoate (0.6 mL, 5.4 mmol) was added into the tube and was stirred for 3 days under room temperature. The product was dialyzed with acetone to remove the methyl-3-mercapto-propanoate, the product **P1S** was obtained after evaporating the solvent and the yield was 86.1%. ^{1}H NMR (500 MHz, $CDCl_3$), δ (TMS, ppm): 7.20–5.84, 3.85, 3.70, 2.80, 2.63, 2.05–1.39, 1.27, 1.05–0.15. ^{13}C NMR (125 MHz, $CDCl_3$), δ (ppm): 172.5, 157.1, 131.7, 130.2, 128.3, 113.2, 70.8, 67.8, 52.3, 38.4, 34.9, 32.2, 29.2, 26.7, 22.8, 20.7, 14.8.

For **P2S**, all the experimental procedures were similar to that for **P1S**, except the reaction time was shortened to 1 day. The yield of **P2S** was 100%. ^{1}H NMR (500 MHz, $CDCl_3$), δ (TMS, ppm): 7.10–5.81, 3.75, 3.25–2.56, 1.25–0.20. ^{13}C NMR (125 MHz, $CDCl_3$), δ (ppm): 172.5, 157.1, 131.7, 130.2, 128.3, 113.2, 70.8, 67.8, 52.3, 38.4, 34.9, 32.2, 29.2, 26.7, 22.8, 20.7, 14.8.

Michael addition reaction. The Michael addition reaction between the amino group of amine and the activated double bond in the polymer side chains was shown in Scheme 3. The experimental procedures for preparation of **P2N** are given below. Into a 10 mL Schlenk tube with 21 mg (0.1 mmol) **P2** dissolved in 2 mL freshly distilled THF. *n*-Butylamine (0.01 mL, 0.1 mmol) was added into the tube and was stirred for 1 day at room temperature. The mixture was precipitated into 300 mL hexane under stirring. The precipitate was allowed to stand overnight and then collected by filtration. The polymer was washed with hexane for several times and dried at room temperature to a constant weight. The yield of polymer **P2N** was 89.4%. The molecular weight is unavailable because the purified **P2N** cannot be dissolved in common solvents including chloroform, dichloromethane, toluene, THF, *N*,*N*-dimethylformamide (DMF), dimethylsulfone (DMSO) and water. We also tried the reaction of **P1** with *n*-butylamine, but no compound could be separated and collected from the reaction mixture.

Conclusion

In summary, PDSAs (**P1** and **P2**) with reactive vinyl groups on their side chains have been synthesized. By using the thiol–ene click reaction, **P1** and **P2** were then modified with mercapto compound to give rise to novel PDSAs (**P1S** and **P2S**) in good yield. The chemical structures of the monomers and polymers were carefully characterized by standard spectroscopic methods such as GPC, ^{1}H NMR, ^{13}C NMR and FTIR techniques, and the data sufficiently supported the availability of the synthetic routes of post-polymerization modification. For P1, the vinyl group at the end of side chain is linked to a saturated alkyl segment, thus the modification of **P1** cost a long reaction time (3 days) to finish the conversion from **P1** to **P1S**. For **P2**, the ene group is an α,β-unsaturated moiety, thus the conversion from **P2** to **P2S** covered a much shorter period (1 day) under mild conditions. Moreover, the activated end-ene group can also react with primary amine, allowing the post-polymerization modification of **P2** with Michael addition. Butylamine was used as a representative of amine compounds to validate the feasibility of the Michael addition route, and the characterization data of **P2N** confirmed the validity for **P2**, but this route was impassable for **P1**. The thermal analysis results indicated that the modified polymers were highly thermally stable, except **P2N**, which showed lower stability due to the imine groups. We also

found that all of the derived polymers were fluorescent, both **P1S** and **P2S** had comparable emission efficiency to their precursors **P1** and **P2**. Besides the synthetic routes of the activated ester and azide-yne click reaction, the thiol–ene click reaction and Michael addition reaction have been demonstrated to be accessible paths to new functional PDSAs.

Acknowledgements

This work was partially supported by the National Basic Research Program of China (973 Program; 2013CB834704) and the National Science Foundation of China (51273175); the Research Grants Council of Hong Kong (604711, 602212 and HKUST2/CRF/10). J. Z. Sun thanks the Jiangsu Key Laboratory of Advanced Functional Polymer Design and Application (Soochow University) for its support.

Notes and references

1 J. W. Y. Lam and B. Z. Tang, *Acc. Chem. Res.*, 2005, **38**, 745.
2 T. Masuda, *J. Polym. Sci., Part A: Polym. Chem.*, 2007, **45**, 165.
3 J. G. Rudick and V. Percec, *Acc. Chem. Res.*, 2008, **41**, 1641.
4 K. Akagi, *Chem. Rev.*, 2009, **109**, 5354.
5 J. Z. Liu, J. W. Y. Lam and B. Z. Tang, *Chem. Rev.*, 2009, **109**, 5799.
6 E. Yashima, K. Maeda, H. Iida, Y. Furusho and K. Nagai, *Chem. Rev.*, 2009, **109**, 6102.
7 B. M. Rosen, C. J. Wilson, D. A. Wilson, M. Peterca, M. R. Imam and V. Percec, *Chem. Rev.*, 2009, **109**, 6275.
8 M. Shiotsuki, F. Sanda and T. Masuda, *Polym. Chem.*, 2011, **2**, 1044.
9 J. Z. Sun, A. Qin and B. Z. Tang, *Polym. Chem.*, 2013, **4**, 211.
10 W. F. Li, H. J. Huang, Y. Li and J. P. Deng, *Polym. Chem.*, 2014, DOI: 10.1039/C3PY01031G.
11 K. A. Gunay, P. Theato and H.-A. Klok, *J. Polym. Sci., Part A: Polym. Chem.*, 2013, **51**, 1.
12 J. Hua, Z. Li, J. W. Y. Lam, H. P. Xu, J. Z. Sun, Y. P. Dong, Y. Q. Dong, A. Qin, W. Z. Yuan, H. Chen, M. Wang and B. Z. Tang, *Macromolecules*, 2005, **38**, 8127.
13 J. Hua, J. W. Y. Lam, Z. Li, A. Qin, J. Z. Sun, Y. Q. Dong, Y. P. Dong and B. Z. Tang, *J. Polym. Sci., Part A: Polym. Chem.*, 2006, **44**, 3538.
14 H. P. Xu, J. Z. Sun, A. Qin, J. Hua, Z. Li, Y. Q. Dong, H. Xu, W. Z. Yuan, Y. Ma, M. Wang and B. Z. Tang, *J. Phys. Chem. B*, 2006, **110**, 20701.
15 Z. Li, Y. Q. Dong, A. Qin, J. W. Y. Lam, Y. P. Dong, W. Z. Yuan, J. Z. Sun, J. Hua, K. S. Wong and B. Z. Tang, *Macromolecules*, 2006, **39**, 467.
16 A. C. Pauly and P. Theato, *J. Polym. Sci., Part A: Polym. Chem.*, 2011, **49**, 211.
17 X. A Zhang, M. R. Chen, H. Zhao, Y. Gao, Q. Wei, S. Zhang, A. Qin, J. Z. Sun and B. Z. Tang, *Macromolecules*, 2011, **44**, 6724.
18 X. A Zhang, A. Qin, L. Tong, H. Zhao, Q. Zhao, J. Z. Sun and B. Z. Tang, *ACS Macro Lett.*, 2012, **1**, 75.
19 A. C. Pauly and P. Theato, *Polym. Chem.*, 2012, **3**, 1769.
20 A. C. Pauly and P. Theato, *Macromol. Rapid Commun.*, 2013, **34**, 516.
21 H. C. Kolb, M. G. Finn and K. B. Sharpless, *Angew. Chem. Int. Ed.*, 2001, **40**, 2004; *Angew. Chem.*, 2001, **113**, 2056.
22 W. H. Binder and R. Sachsenhofer, *Macromol. Rapid Commun.*, 2007, **28**, 15.
23 A. Qin, J. W. Y. Lam and B. Z. Tang, *Chem. Soc. Rev.*, 2010, **39**, 2522.
24 M. G. Finn and V. V. Fokin, *Chem. Soc. Rev.*, 2010, **39**, 1231.
25 C. E. Hoyle and C. N. Bowman, *Angew. Chem., Int. Ed.*, 2010, **49**, 1540.
26 W. Z. Yuan, A. Qin, J. W. Y. Lam, J. Z. Sun, M. Haussler, J. Liu, H. P. Xu, Q. Zheng and B. Z. Tang, *Macromolecules*, 2007, **40**, 3159.
27 L. Tong, A. Qin, X. A Zhang, Y. Mao, J. Z. Sun and B. Z. Tang, *Sci. China: Chem.*, 2011, **12**, 1948.
28 T. Masuda, B. Z. Tang, T. Higashimura and H. Yamaoka, *Macromolecules*, 1985, **18**, 2369.
29 W. Z. Yuan, J. Z. Sun, Y. Dong, M. Haussler, F. Yang, H. P. Xu, A. Qin, J. W. Y. Lam, Q. Zheng and B. Z. Tang, *Macromolecules*, 2006, **39**, 8011.
30 J. L. Hua, J. W. Y. Lam, H. Dong, L. Wu, K. S. Wong and B. Z. Tang, *Polymer*, 2006, **47**, 18.
31 J. W. Y. Lam and B. Z. Tang, *J. Polym. Sci., Part A: Polym. Chem.*, 2003, **41**, 2607.
32 A. C. Grimsdale, K. L. chan, R. E. Martin, P. G. Jokisz and A. B. Holmes, *Chem. Rev.*, 2009, **109**, 897.
33 J. W. Y. Lam, J. D. Luo, Y. Dong, K. K. L. Cheuk and B. Z. Tang, *Macromolecules*, 2002, **35**, 8288.
34 A. Qin, C. K. W. Jim, Y. H. Tang, J. W. Y. Lam and B. Z. Tang, *J. Phys. Chem. B*, 2008, **112**, 9281.
35 Y. Hong, J. W. Y. Lam and B. Z. Tang, *Chem. Soc. Rev.*, 2011, **40**, 5361.
36 Y. Hong, J. W. Y. Lam and B. Z. Tang, *Chem. Commun.*, 2009, 4332.